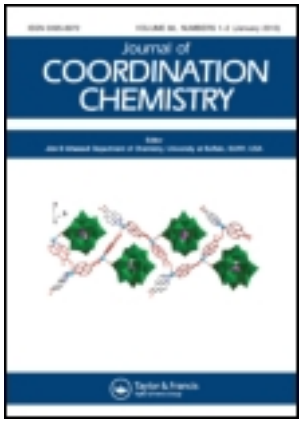

Journal of Coordination Chemistry
Publication details, including instructions for authors and subscription information:
http://www.tandfonline.com/loi/gcoo20

Synthesis, crystal structure, and biological activity of a nickel(II) complex constructed by 2-phenyl-4-selenazole carboxylic acid and 1,10-phenanthroline

Bao-Bao Xu [a], Pei Shi [b], Quan-Yin Guan [b], Xia Shi [b] & Guo-Liang Zhao [a b]

[a] Xingzhi College, Zhejiang Normal University, Jinhua, China
[b] College of Chemistry and Life Sciences, Zhejiang Normal University, Jinhua, China

Accepted author version posted online: 07 Jun 2013.Published online: 08 Jul 2013.

To cite this article: Bao-Bao Xu, Pei Shi, Quan-Yin Guan, Xia Shi & Guo-Liang Zhao (2013) Synthesis, crystal structure, and biological activity of a nickel(II) complex constructed by 2-phenyl-4-selenazole carboxylic acid and 1,10-phenanthroline, Journal of Coordination Chemistry, 66:15, 2605-2614, DOI: 10.1080/00958972.2013.811497

To link to this article: http://dx.doi.org/10.1080/00958972.2013.811497

Journal of Coordination Chemistry, 2013
Vol. 66, No. 15, 2605–2614, http://dx.doi.org/10.1080/00958972.2013.811497

Synthesis, crystal structure, and biological activity of a nickel (II) complex constructed by 2-phenyl-4-selenazole carboxylic acid and 1,10-phenanthroline

BAO-BAO XU†, PEI SHI‡, QUAN-YIN GUAN‡, XIA SHI‡ and GUO-LIANG ZHAO*†‡

†Xingzhi College, Zhejiang Normal University, Jinhua, China
‡College of Chemistry and Life Sciences, Zhejiang Normal University, Jinhua, China

(*Received 14 November 2012; in final form 18 April 2013*)

A nickel(II) complex, $[NiL(phen)_2]L\cdot 5H_2O$ (HL = 2-phenyl-4-selenazole carboxylic acid, $C_{10}H_7O_2NSe$, phen = 1,10-phenanthroline), was synthesized and characterized by elemental analysis and IR. The single crystal structure was determined by single-crystal X-ray diffraction. $C_{88}H_{78}N_{12}Ni_2O_{19}Se_4$ crystallized in the triclinic system, space group $P\bar{1}$. The interaction between the complex and the calf thymus DNA was studied by an ethidium bromide fluorescent probe. The antibacterial activities of the complex and ligand against five species of bacteria, *Escherichia coli*, *Staphylococcus epidermidis*, *Streptococcus viridans*, *Staphylococcus aureus* and *Acinetobacter baumanii*, were tested. The anticancer activities of the complex against human pancreatic cancer line PANC-28 and human hepatocarcinoma line HuH7 were also studied by employing an MTT assay.

Keywords: Nickel(II) complex; 2-Phenyl-4-selenazole carboxylic acid; Biological activity; Crystal structure; 1, 10-Phenanthroline

1. Introduction

Nickel is a necessary microelement for organisms, an activator for many enzymes, such as arginase, acid phosphatase, decarboxylase, deoxyribonuclease and peptidase, and promotes cytopoiesis [1]. Structural study of nickel complexes associated with molecular magnets, biological activities, and catalysis has been reported [2–4]. Selenium is also a necessary microelement for vital movement. Selenium plays significant roles [1, 5–7] in tumor prevention and treatment, antioxidation, antiaging, protecting the heart, relieving the side reaction caused by chemotherapy drugs, increasing drug tolerance, reducing cisplatin nephrotoxicity, and ototoxicity, as well as maintaining normal endocrine function. Since the 1980s, a large number of bioactive organoselenium compounds have been synthesized with selenazole derivatives exhibiting especially favorable antitumor and antibacterial activities. This indicates that they are potentially useful as drugs and drug intermediates. Srivastava and Boritzki [8, 9] found that selenazofurin was a highly efficient antiviral and antitumor drug, and exhibited significant *in vitro* inhibitory activity against lymphoblastic

*Corresponding author. Email: sky53@zjnu.cn

leukemia diseased cells P338 and L1210. Kumar [10, 11] found that some selenazole derivatives exhibited anti-proliferative activity against L1210 cells *in vitro*. Ito [12] found that 6-phenyl-7(6H)-isoselenazolo[4,3-d]pyrimidone inhibited the growth of mouse Ehrlich ascites tumor *in vivo* and 4,5-dihydro-4-methyl-6-oxo-5-phenyl-6H-pyrazolo[4,5-c] isoselenazole was shown to exhibit inhibitory activity against mouse Ehrlich ascites tumor as well.

Research about selenazole complexes is still rare. There are a few reports [13–17] concentrating on synthesis and structural studies. We have reported the synthesis and biological activity assay of some 2-phenyl-4-selenazole carboxylic acid binary complexes [18, 19]. In continuation of our efforts in this area, a nickel(II) complex, $[NiL(phen)_2]L{\cdot}5H_2O$, was synthesized and characterized, and its crystal structure was reported. The interaction intensity and mode between the title complex and the DNA had been examined by an ethidium bromide (EB) fluorescent probe and reported with their antibacterial and anticancer activities.

2. Experimental

2.1. *Materials and methods*

Escherichia coli, *Staphylococcus epidermidis*, *Streptococcus viridans*, *Staphylococcus aureus*, and *Acinetobacter baumanii* were supplied by the Jinhua Municipal Hospital of Zhejiang Province. Human cancer lines, PANC-28 and HuH7, were purchased from the Shanghai Institute of Cellular Biology of the Chinese Academy of Sciences. All other solvents and reagents were purchased as analytical grade from commercial sources and used without purification. Elemental analyses (C, H, N) were carried out on a Vario EL III elemental analyzer. The metal contents were determined by an EDTA complexometric titration after decomposing a known amount of the complex with concentrated nitric acid. The IR spectrum was recorded on a Nicolet NEXUS-670 FTIR spectrometer with a KBr pellet from 400∼4000 cm^{-1}. Single-crystal X-ray diffraction data were obtained on a Bruker Smart APEXII-CCD diffractometer. The optical density (OD) was measured with a Perkin-Elmer LS55 spectrophotometer.

2.2. *Synthesis of the complex*

The ligand was obtained by a reported procedure [18]. A mixture of $Ni(OH)_2$ (1 mmol, 0.093 g), HL (2 mmol, 0.45 g), phen (2 mmol, 0.396 g), and H_2O (40 mL) was sealed in a 50 mL stainless steel reactor with a Teflon liner and heated to 120 °C for 72 h under autogenous pressure, and then cooled to room temperature. The mixture was filtered, giving red single crystals suitable for X-ray analysis in 37% yield (based on Ni). IR (KBr, cm^{-1}): 3449, 3105, 1606, 1514, 1459, 1422, 1362, 861, and 734. Elemental Anal. Calcd for $C_{88}H_{78}N_{12}Ni_2O_{19}Se_4$ (%): C, 51.79; H, 3.85; N, 8.24. Found: C, 51.61; H, 3.82; N, 8.29.

2.3. *Fluorescence quenching experiments*

The interaction of the complex with calf thymus DNA (CT-DNA) was studied by an EB fluorescent probe. The experiment was carried out by adding different volumes of complex solution (10^{-4} mol L^{-1}) to a 10 mL colorimetric cylinder prepared 2 h in

advance, which contained 2.0 mL 100 μg mL^{-1} EB, 1.0 mL 200 μg mL^{-1} CT-DNA, and 2.0 mL tris-HCl buffer solution (pH 7.4), then the mixed solutions were diluted with double-distilled water. The final solutions were incubated for 12 h at 4 °C. The fluorescence was recorded at an excitation wavelength of 251 nm and emission wavelength between 520 and 700 nm.

2.4. *Antimicrobial and anticancer activity assays*

Growth of the cultures was monitored on a spectrophotometer by measuring the OD of bacterium suspensions at 600 nm. The inhibition ratio of compounds against bacteria was calculated as follows: inhibition ratio (%) = (1-OD_a/OD_b) × 100%, where OD_a and OD_b represent the OD of bacterium suspensions in the absence and presence of compounds, respectively. Benzylpenicillin sodium and ciprofloxacin were used for comparison. All experiments were performed in triplicate and the data are mean values with a standard deviation (SD).

The anticancer activities of compounds against human pancreatic cancer line PANC-28 and human hepatocarcinoma line HuH7 were studied by employing MTT assay following standard procedure [20]. Each experiment was carried out on at least three separate occasions and the data are mean values ±SD. Cis-platinum (Cis-Pt) was used as the comparison.

2.5. *Crystallographic study*

A single crystal of the complex with approximate dimensions 0.318 mm × 0.133 mm × 0.048 mm was mounted on a Bruker Smart Apex CCD diffractometer. The diffraction data were collected using graphite-monochromated Mo Kα radiation (λ = 0.71073 Å) at 296(2) K. Absorption corrections were applied using SADABS [21]. The structure was solved using SHELXS-97 [22] and refined with full-matrix least-squares method based on F^2 using SHELXTL-97 [23]. Remaining hydrogens were added in calculated positions and refined as riding with a common fixed isotropic thermal parameter. Hydrogens on water were located in a difference Fourier map and included in the subsequent refinement using restraints (d(O–H) = 0.85 Å and d(H···H) = 1.30 Å) with U_{iso}(H) = 1.5 U_{eq}(O). Other hydrogens were added theoretically. The crystallographic data of the complex is given in table 1. Selected bond distances and angles are listed in table 2.

3. Results and discussion

3.1. *IR spectra*

The broad absorption at 3449 cm^{-1} can be assigned to water, which confirms the presence of water in the complex. Two absorptions at 1422 cm^{-1} ($\nu_{as(COO-)}$) and 1362 cm^{-1} ($\nu_{a(COO-)}$) show coordination of carboxylate with Ni^{2+}. Three bands at 1514 cm^{-1} ($\delta_{C=N}$), 861 cm^{-1} (δ_{C-C}), and 734 cm^{-1} (δ_{C-H}) support coordination of nitrogen from phen. The appearance of an intense antisymmetric carboxylate stretching group υ_{as}(–coo$^-$) and a

Table 1. Crystal data of the complex.

Empirical formula	$C_{44}H_{38}N_6NiO_9Se_2$
Formula weight	1101.43
Temperature (K)	296(2)
Crystal system	Triclinic
Space group	$P\bar{1}$
a (Å)	12.8991(9)
b (Å)	13.1954(4)
c (Å)	14.1474(5)
α (°)	116.068(2)
β (°)	96.007(3)
γ (°)	97.901(3)
V (Å^3)	2105.33(18)
Z	2
Dc (g cm^{-3})	1.596
Absorption coefficient (mm^{-1})	2.254
Crystal size (mm)	0.318 × 0.133 × 0.048
Crystal color	Pnk
F (000)	1024
Reflections collected	29,007
Unique reflections	7371
Observable reflections	5089
θ_{min}, θ_{max} (°)	1.63, 24.99
Final R indices [$I > 2\sigma(I)$]	$R_1 = 0.0470$, $wR_2 = 0.1203$
R indices (all data)	$R_1 = 0.0793$, $wR_2 = 0.1333$
Goodness-of-fit (on F^2)	1.005
$\Delta\rho$ max, $\Delta\rho$ min (e nm^{-3})	1.517, −0.453

Table 2. Selected bond distances (Å) and angles (°) of the complex.

Ni1–O4	2.035(3)
Ni1–N5	2.075(4)
Ni1–N6	2.080(3)
Ni1–N3	2.103(4)
Ni1–N4	2.113(3)
O(4)–Ni(1)–N(5)	93.98(13)
O(4)–Ni(1)–N(6)	174.06(13)
N(5)–Ni(1)–N(6)	80.09(14)
O(4)–Ni(1)–N(3)	89.25(12)
N(5)–Ni(1)–N(3)	91.58(14)
N(6)–Ni(1)–N(3)	91.21(13)
O(4)–Ni(1)–N(4)	95.01(12)
N(5)–Ni(1)–N(4)	167.29(14)
N(6)–Ni(1)–N(4)	90.90(13)
Ni(1)–N(2)	2.126(3)
Se1–C7	1.879(5)
Se1–C8	1.843(5)
Se2–C17	1.875(4)
Se2–C18	1.827(4)
N(3)–Ni(1)–N(4)	79.57(14)
O(4)–Ni(1)–N(2)	80.46(12)
N(5)–Ni(1)–N(2)	97.52(14)
N(6)–Ni(1)–N(2)	99.91(13)
N(3)–Ni(1)–N(2)	166.67(13)
N(4)–Ni(1)–N(2)	92.82(13)
C(18)–Se(2)–C(17)	85.6(2)
C(8)–Se(1)–C(7)	83.7(2)

symmetric carboxylate stretching group υ_s(–coo$^-$) at about 1606 cm^{-1} and 1459 cm^{-1} are assigned to free L^{-1}. These results [24] are confirmed by X-ray diffraction analysis.

3.2. *Crystal structure descriptions*

Single-crystal X-ray diffraction reveals that the complex crystallizes in the triclinic space group $P\bar{1}$, whereby the basic coordination unit contains one $[NiL(phen)_2]^+$, one free L^{-1}, and five uncoordinated waters (figure 1). Ni^{2+} is coordinated by N2, N3, N4, N5, and N6 from two phen ligands and L^- and O4 from L^{-1}, forming a slightly distorted octahedral geometry. The Ni–O bond distance is 2.035(3) Å and the Ni–N bond distances range from 2.075(4) to 2.126(3) Å, similar to $[Ni(pydc)(bipy)_2]\cdot 7H_2O$ [25]. The angle formed by the mean planes of the two phen ligands is 83.820(87)°.

Weak bonding interactions are important in the formation of these types of structures. In this complex, hydrogen bonds (table 3) between adjacent molecules form a cyclic dimer, in which two $[NiL(phen)_2]^+$ and two L^{-1} are in angular positions, respectively. O1 and O2 from free L^{-1} connect O3 W and O2 W, respectively, via weak bonding interactions (O3 W-H3WB···O1^i, O2 W-H2WA···O2^i, symmetry code: $i-x+1, -y+1, -z+1$), then bridge $[NiL(phen)_2]^+$ through O–H···O hydrogen bonds with O···O distances of 2.824(7) to 2.922(9) Å. The Se2···O1 W and Se1···O1 W distances are 3.013 Å and 3.129 Å, respectively, which are longer than a single Se–O binding distance [26,27] and much shorter than the sum of the van der Waals radii between Se and O (3.42 Å). This indicates weak intermolecular interactions between selenium and oxygen, supporting hydrogen bonding interactions influencing the Se–O intermolecular interactions in the crystal packing

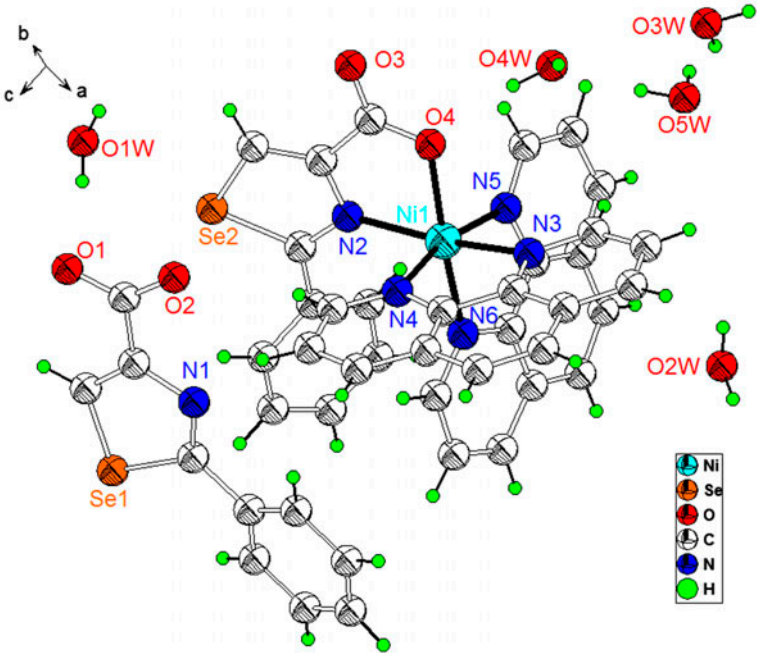

Figure 1. Molecular structure of the complex.

Table 3. Hydrogen bond intermolecular interactions for the complex.

D-H···A	d(D-H) (Å)	d(H···A) (Å)	d(D···A) (Å)	∠DHA (°)
O(1 W)-H(1 WA)···O(1)	0.85	2.00	2.831(5)	167.1
O(1W)-H(1WB)···O(3)^{i}	0.85	2.01	2.861(5)	179.8
O(2 W)-H(2 WA)···O(2)^{ii}	0.85	1.89	2.741(5)	179.6
O(2W)-H(2WB)···O(3)^{iii}	0.85	2.06	2.908(5)	179.6
O(3 W)-H(3WA)···O(2 W)^{iv}	0.85	1.97	2.824(7)	178.9
O(3 W)-H(3WB)···O(1)^{v}	0.85	1.94	2.788(7)	178.9
O(4 W)-H(4WA)···O(4)	0.85	1.99	2.840(7)	173.4
O(5 W)-H(5WA)···O(3 W)	0.85	2.08	2.922(9)	170.7
O(5 W)-H(5WB)···O(4 W)	0.85	1.97	2.798(12)	165.9

Symmetry codes: $^{i}-x+1,-y+1,-z+1$; $^{ii}-x+2,\ -y+1,\ -z+1$; $^{iii}x+1,\ y,\ z$; $^{iv}-x+2,\ -y,\ -z$; $^{v}x,\ y-1,\ z-1$.

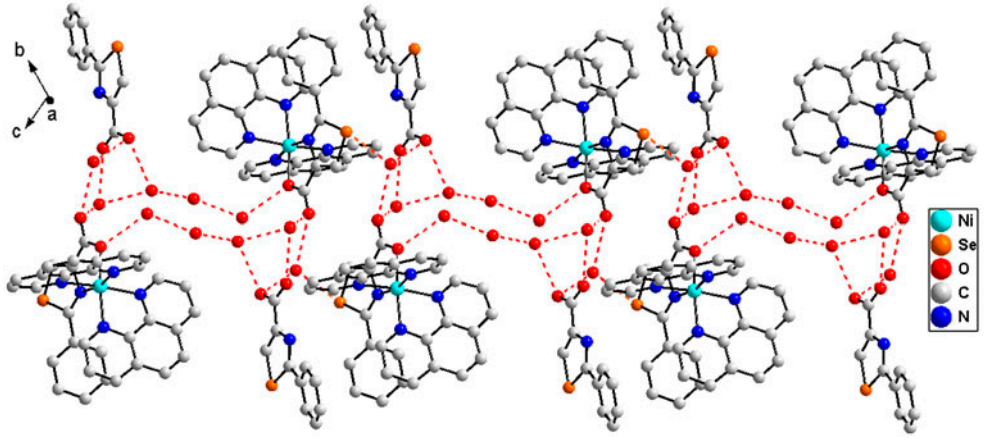

Figure 2. Packing diagram of the complex viewed along the *a* axis displaying a 1-D chain. Hydrogen bond intermolecular interactions and weak bonds are shown as dashed lines. Hydrogens not involved in hydrogen bonding have been removed for clarity.

of the structure. Due to hydrogen bonds, adjacent cyclic dimers form a 1-D chain (figure 2) along the *a* axis. Additional H-bonds link adjacent chains forming a 2-D network (figure 3).

3.3. *EB displacement experiment*

Figure 4 shows emission spectra of the DNA-EB system with increasing amounts of the complex. The complex shows no fluorescence at 592 nm, while DNA-bound EB solution exhibits strong fluorescence. When the complex is added to DNA-bound EB solution, a substantial decrease in emission intensities is observed on increase in concentration of the complex. This indicates the intercalation of the complex into DNA. From spectral data, the quenching parameter can be calculated according to the Stern–Volmer equation [28]: $I_0/I = 1 + K_{sq}r$, where I_0 and I are the emission intensities in the absence and presence of the complex, respectively. K_{sq} is the quenching constant and r is the concentration ratio of the complex to DNA. K_{sq} can be obtained as slope from the plot of I_0/I versus r linear plot. The K_{sq} value of 4.78 indicates strong intercalation of the complex into DNA.

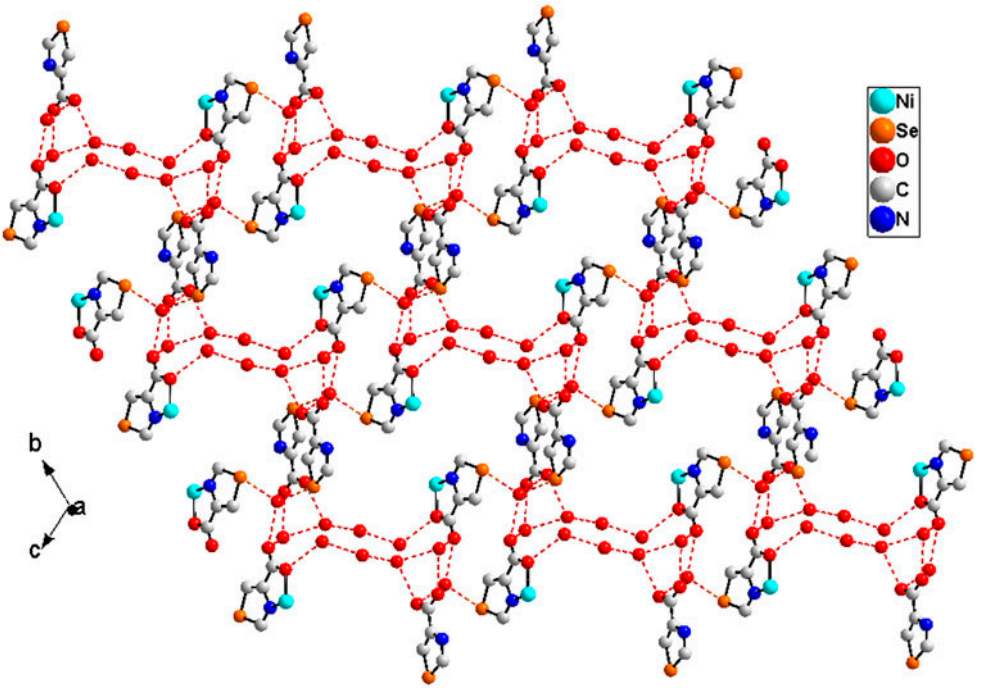

Figure 3. Packing diagram of the complex viewed along the *a* axis displaying a 2-D network. Hydrogen bond intermolecular interactions and weak bonds are shown as dashed lines. Hydrogens not involved in hydrogen bonding have been removed for clarity.

3.4. *Antimicrobial activity*

The antimicrobial activity results (figure 5) of four compounds (benzylpenicillin sodium, ciprofloxacin, ligand, and complex) in two concentrations (1.0×10^{-3} mol L^{-1} and 1.0×10^{-4} mol L^{-1}) against *E. coli*, *S. epidermidis*, *S. viridans*, *S. aureus,* and *A. baumanii* are presented. At 1.0×10^{-4} mol L^{-1}, the complex and ligand slightly inhibit the growth of the five test bacteria. At 1.0×10^{-3} mol L^{-1}, the complex exhibits stronger inhibition against *E. coli*, *S. viridans,* and *A. baumanii,* but weaker activity against *S. epidermidis* and *S. aureus* than the ligand. The inhibition activity of the complex against *E. coli*, *S. epidermidis,* and *S. Viridans* is stronger than benzylpenicillin sodium, but weaker than ciprofloxacin. The inhibition activity of the complex against *S. aureus* is a little stronger than ciprofloxacin, but much weaker than benzylpenicillin sodium. The complex strongly inhibits the growth of *A. baumanii* and the intensity is much higher than benzylpenicillin sodium and ciprofloxacin.

3.5. *Anticancer activity*

The complex and ligand were examined for *in vitro* anticancer activities against human cancer lines PANC-28 and HuH7. The IC_{50} values of the two tested compounds, as well as Cis-Pt, included as comparison, are listed in table 4. The results indicate that the ligand

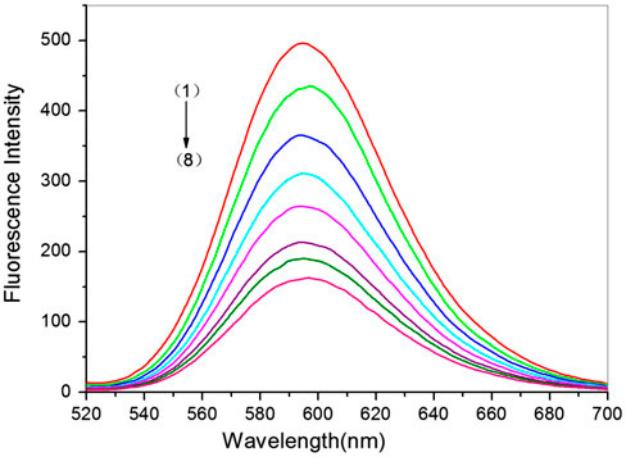

Figure 4. Emission spectra of EB-DNA system in the absence and presence of the complex, from 1 to 8: r = [compound]/[DNA] = 0, 0.067, 0.13, 0.20, 0.27, 0.34, 0.40, 0.47, respectively.

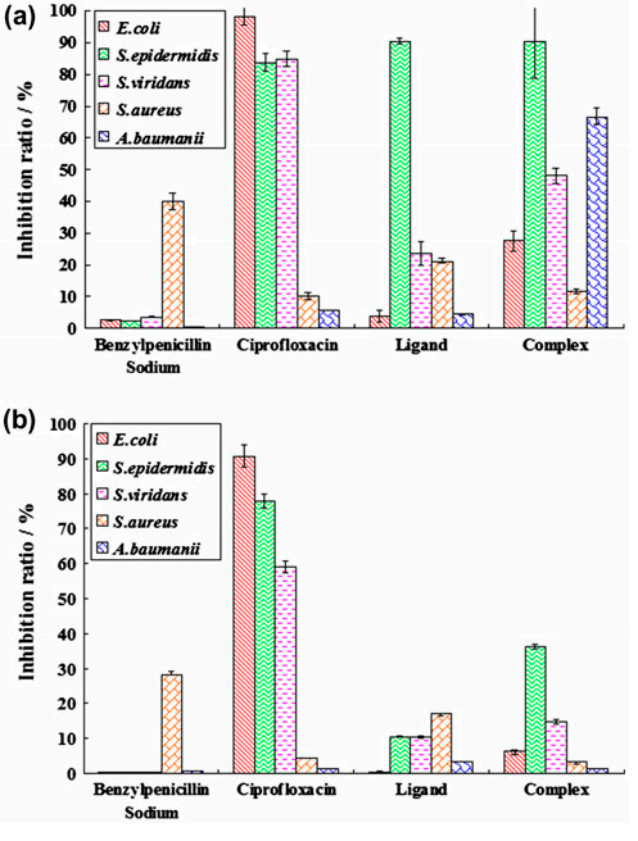

Figure 5. Inhibition ratio of compounds against five species of bacteria (%, $\bar{x}$ ±SD), (a) [compound] = 1.0×10^{-3} mol L^{-1}; (b) [compound] = 1.0×10^{-4} mol L^{-1}.

Table 4. Inhibitory effects of compounds on cancer cell proliferation *in vitro* ($\bar{x}$ ±SD).

	Cell lines (IC_{50}/μ mL^{-1})	
Compounds	PANC-28	HuH7
Ligand	863.572 ± 0.012	1563.570 ± 0.032
Complex	30.07 ± 0.041	361.25 ± 0.026
Cis-Pt	10.240 ± 0.002	19.220 ± 0.001

does not show inhibitory effect against the above two cancer lines. The inhibitory effect of the complex against HuH7 was common and much weaker than Cis-Pt. However, the complex exhibited good inhibitory effect against cancer line PANC-28, slightly weaker than observed for Cis-Pt.

4. Conclusions

A nickel(II) ternary complex containing 2-phenyl-4-selenazole carboxylic acid and phen has been synthesized and characterized. The interaction of the complex with CT-DNA has been investigated by the EB fluorescent probe. Our results indicate that the intercalation of the complex into CT-DNA is very strong, suggesting that the large rigid aromatic ring plane of phen increases insertion ability. The biological activities of the complex have been evaluated by antimicrobial and anticancer assay. The complex exhibits stronger antimicrobial activities than benzylpenicillin sodium.

Supplementary material

CCDC No. 803434 of the complex contains the supplementary crystallographic data for this paper. The data can be obtained free of charge from the Cambridge Crystallographic Data Centre via http://www.ccdc.cam.ac.uk/conts/retrieving.html (or from the CCDC, 12 Union Road, Cambridge CB2 1EZ, UK; Fax: +44 1223 3360-33; E-mail: deposit@ccdc.cam.ac.uk).

Acknowledgment

This work was financially supported by the Natural Science Foundation of Zhejiang Province (Y4080256).

References

[1] K.-D. Yang. *Microelement and Health*, Science Press, Beijing (2003).
[2] S.M. Humphrey, R.A. Mole, M. McPartlin, E.J.L. Mclnnes, P.L. Wood. *Inorg. Chem.*, **44**, 5981 (2005).
[3] Y. Ding, Z.H. Zhang, Z.Q. Hu, Z.J. Ku. *Chin. J. Inorg. Chem.*, **22**, 1187 (2006).
[4] Y. Bai, D.B. Dang, C.Y. Duan. *Chin. J. Inorg. Chem.*, **21**, 1155 (2005).
[5] B.H. Xu, Y. Sun. *Chin. J. New Drugs*, **7**, 176 (1998).
[6] L. Letavayová, V. Vlčková, J. Brozmanová. *Toxicology*, **227**, 1 (2006).
[7] M.A. Lovell, S.L. Xiong, G. Lyubartseva, W.R. Markesbery. *Free Radical Biol. Med.*, **46**, 1527 (2009).
[8] P.C. Srivastava, R.K. Robins. *J. Med. Chem.*, **26**, 445 (1983).

[9] T.J. Boritzki, D.A. Berry, J.A. Besserer, P.D. Cook, D.W. Fry, W.R. Leopold, R.C. Jackson. *Biochem. Pharmacol.*, **34**, 1109 (1985).
[10] Y. Kumar, R. Green, K.Z. Borysko, D.S. Wise, L.L. Wotring, L.B. Townsend. *J. Med. Chem.*, **36**, 3843 (1993).
[11] Y. Kumar, R. Green, D.S. Wise, L.L. Wotring, L.B. Townsend. *J. Med. Chem.*, **36**, 3849 (1993).
[12] H. Ito, J. Sakakibara, T. Ueda. *Cancer Lett.*, **28**, 61 (1985).
[13] E. Ruiz, X.Y. Tang, X.J. Li, M.M. Muir. *J. Crystallogr. Spectrosc. Res.*, **23**, 791 (1993).
[14] M.M. Muir, G.M. Gomez, M.E. Cadiz, J.A. Muir. *Inorg. Chim. Acta*, **168**, 47 (1990).
[15] K.M. Barkigia, M.W. Renner, M.O. Senge, J. Fajer. *J. Phys. Chem. B*, **108**, 2173 (2004).
[16] A.J. Zhou, S.L. Zheng, Y. Fang, M.L. Tong. *Inorg. Chem.*, **44**, 4457 (2005).
[17] C.K. Tan, J. Wang, J.D. Leng, L.L. Zheng, M.L. Tong. *Eur. J. Inorg. Chem.*, **2008**, 771 (2008).
[18] G.L. Zhao, X. Shi, J.P. Zhang, J.F. Liu, H.D. Xian, L.X. Shao. *Sci. Sin. Chim.*, **40**, 1525 (2010).
[19] G.L. Zhao, J.B. Shen, X. Shi, J.F. Chen, X. Lv, Y.F. Zhou, Y. Chen. *Chin. J. Inorg. Chem.*, **28**, 959 (2012).
[20] A. Kamal, A. Mallareddy, P. Suresh, V.L. Nayak, R.V.C.R.N.C. Shetti, N.S. Rao, J.R. Tamboli, T.B. Shaik, M.V.P.S. Vishnuvardhan, S. Ramakrishna. *Eur. J. Med. Chem.*, **47**, 530 (2012).
[21] G.M. Sheldrick. *SADABS, Program for Empirical Absorption Correction of Area Detector Data*, University of Göttingen, Germany (1997).
[22] G.M. Sheldrick. *SHELXS 97, Program for Crystal Structure Solution*, University of Göttingen, Germany (1997).
[23] G.M. Sheldrick. *SHELXL 97, Program for Crystal Structure Refinement*, University of Göttingen, Germany (1997).
[24] K. Nakamoto. *Infrared and Raman Spectra of Inorganic and Coordination Compounds*, 4th Edn, Wiley, New York (1986).
[25] A.T. Çolak, D. Akduman, O.Z. Yeşilel, O. Büyükgüngör. *Transition Met. Chem.*, **34**, 861 (2009).
[26] R.O. Day, R.R. Holmes. *Inorg. Chem.*, **20**, 3071 (1981).
[27] T.M. Klapötke, B. Krumm, K. Polborn. *Eur. J. Inorg. Chem.*, **1999**, 1359 (1973).
[28] J.R. Lakowicz, G. Weber. *Biochemistry*, **12**, 4161 (1973).